Available online at www.sciencedirect.com

SCIENCE DIRECT

ELSEVIER

Journal of Solid State Chemistry 177 (2004) 1431–1436

JOURNAL OF SOLID STATE CHEMISTRY

http://elsevier.com/locate/jssc

Hydrothermal synthesis and structure of $K_6[(UO_2)_4(CrO_4)_7] \cdot 6H_2O$: A layered uranyl chromate with a new uranyl sheet topology

Richard E. Sykora, Steven M. McDaniel, and Thomas E. Albrecht-Schmitt*

Department of Chemistry, Auburn University, 179 Chemistry Building, Auburn, AL 36849, USA

Received 18 September 2003; received in revised form 4 November 2003; accepted 23 November 2003

Abstract

The layered uranyl chromate, $K_6[(UO_2)_4(CrO_4)_7] \cdot 6H_2O$ (1), has been synthesized by reacting UO_3 with $K_2Cr_2O_7$ under mild hydrothermal conditions. The structure of 1 is formed from UO_2^{2+} cations that are bound by chromate anions to yield a pentagonal bipyramidal geometry around the uranium centers. These polyhedra are bridged by chromate anions to yield one-dimensional $^1_\infty[UO_2(CrO_4)_2]^{2-}$ chains. The chains are similar to the $^1_\infty[UO_2(CrO_4)_2(H_2O)]^{2-}$ chains found in the previously reported one-dimensional uranyl chromate, $K_2[UO_2(CrO_4)_2(H_2O)] \cdot 3H_2O$, a phase that forms concomitantly with 1. These chains are condensed with the loss of the coordinated water molecules into two-dimensional $^2_\infty[(UO_2)_4(CrO_4)_7]^{6-}$ layers with additional one-dimensional $^1_\infty[(UO_2)_2(CrO_4)_3]^{2-}$ chains. These anionic layers form a new type of anionic sheet topology and are charge balanced by both intra- and interlayer K^+ cations. Crystallographic data (193 K): 1, orthorhombic, space group $P2_12_12$, $a = 10.9583(5)$ Å, $b = 22.582(1)$ Å, $c = 7.9552(4)$ Å, $Z = 2$, Mo$K\alpha$, $\lambda = 0.71073$, $R(F) = 1.77\%$ for 268 parameters with 4657 reflections with $I > 2\sigma(I)$.

Keywords: Uranyl chromate; Hydrothermal synthesis; Layered structure

1. Introduction

Tetrahedral oxoanions have been shown to form a large number of different structure types with UO_2^{2+} cations, due in part to the versatility by which four binding atoms can coordinate uranyl, and to the differing charges that can be associated with common tetrahedral anions ranging from −1 to −4. $[(CH_3)_4N][(C_5H_5NH)_{0.8}((CH_3)_3NH)_{0.2}][(UO_2)_2Si_9O_{19}F_4]$ [1], $Ag_6[(UO_2)_3O(MoO_4)_5]$ [2], $UO_2(ClO_4)_2(H_2O)_7$ [3], $Ca_2[(UO_2)_3(PO_4)_2(OH)_4] \cdot 4H_2O$ [4], and $Ni[(UO_2)_2(VO_4)_2] \cdot 4H_2O$ [5] are only a few of the U(VI) compounds containing tetrahedral oxoanions that have been either discovered as minerals, or produced synthetically. We have recently reported the hydrothermal preparation and structures of the mixed-metal uranyl iodates, $Rb[UO_2(CrO_4)(IO_3)(H_2O)]$ [6], $A_2[UO_2(CrO_4)(IO_3)_2]$ ($A = K$ [6], Rb [6], Cs [6,7]), and $K_2[UO_2(MoO_4)(IO_3)_2]$ [6], that also contain tetrahedral chromate or molybdate anions, respectively.

A large number of phases have been reported in the uranyl chromate system [8–26]. These compounds have been characterized largely through the use of thermal analysis [8–12] and powder X-ray diffraction [8–16]. Single-crystal structures have been determined for $[NH_4]_2[(UO_2)_2(CrO_4)_3] \cdot 6H_2O$ [17], $K[UO_2(CrO_4)(OH)] \cdot 1.5H_2O$ [18], and $Sr[(UO_2)_2(CrO_4)_2(OH)_2] \cdot 8H_2O$ [19], all of which contain two-dimensional anionic layers. Quite recently, the crystal structures of the one-dimensional uranyl chromates $UO_2(CrO_4)(H_2O)_2$, $[UO_2(CrO_4)(H_2O)_2] \cdot H_2O$, and $[UO_2(CrO_4)(H_2O)_2]_4 \cdot 9H_2O$ were reported [20]. In addition to these purely inorganic phases, several uranyl chromates containing various organic molecules incorporated into their structures have been produced and their structures elucidated [10,13,21–27]. Single-crystal structures of $UO_2(CrO_4)(CONH_2CH_3)_2$ [21], $UO_2(CrO_4)\{CH_3CON(C_2H_5)\}_2$ [22], and $(H_3O)_2[(UO_2)_{12}(CrO_4)_{13}] \cdot 12HCON(CH_3)_2$ [23] reveal that all of these compounds contain organic molecules coordinated directly to the U(VI) centers of uranyl cations, and these ligands play a critical role in determining the structure that is adopted.

Two potassium uranyl chromates, $K_2[(UO_2)_2(CrO_4)_3] \cdot 6H_2O$ [12] and $K_2[UO_2(CrO_4)_2(H_2O)] \cdot 3H_2O$ [8], have been previously reported and formulated

---

*Corresponding author. Fax: +334-844-6959.

E-mail address: albreth@auburn.edu (T.E. Albrecht-Schmitt).

0022-4596/$ - see front matter © 2003 Elsevier Inc. All rights reserved.
doi:10.1016/j.jssc.2003.11.025

by elemental analysis, thermal analysis, and powder X-ray diffraction. Herein we report the structure of a novel two-dimensional phase, $K_6[(UO_2)_4(CrO_4)_7] \cdot 6H_2O$ (1), and make structural comparisons between it and $K_2[UO_2(CrO_4)_2(H_2O)] \cdot 3H_2O$. Compound 1 contains a new anionic sheet topology built in part from the condensation of one-dimensional chains that are similar to those observed in $K_2[UO_2(CrO_4)_2(H_2O)] \cdot 3H_2O$. Both of these compounds have been prepared under mild hydrothermal conditions.

2. Experimental

2.1. Syntheses

UO_3 (99.8%, Alfa-Aesar) and $K_2Cr_2O_7$ (ACS certified, Fisher) were used as received. Distilled and millipore filtered water with a resistance of 18.2 MΩ was used in all reactions. Reactions were run in Parr 4749 23-mL autoclaves with PTFE liners. The reactions reported produced the highest yields of the desired compounds. SEM/EDX analyses were performed using a JEOL 840/Link Isis instrument. K, U, and Cr percentages were calibrated against standards. Typical results are within 3% of actual ratios. IR spectra were collected on a Nicolet 5PC FT-IR spectrometer from KBr pellets. While the UO_3 contains depleted U, standard precautions for handling radioactive materials should be followed. Old sources of U should not be used, as the daughter elements of natural decay are highly radioactive and present serious health risks.

2.2. $K_6[(UO_2)_4(CrO_4)_7] \cdot 6H_2O$ (1)

UO_3 (246 mg, 0.86 mmol) and $K_2Cr_2O_7$ (254 mg, 0.86 mmol) were loaded into an autoclave. Water (1 mL) was then added to the solids. The autoclave was heated at 180°C for 72 h, and slow cooled at 9°C/h to 22°C. Monophasic orange prisms of 1 were located beneath an orange mother liquor. The crystals were rinsed with water and then methanol. Yield for 1: 436 mg (91% based on U). EDX analysis provided a K:U:Cr ratio of 6:4:7. IR (KBr, cm^{-1}): 3374 (ν_{OH}, m, br), 1602 (δ_{OH}, m), 967 (ν_{CrO}, m), 961 (ν_{CrO}, m, sh), 946 (ν_{CrO}, m), 920 (ν_{CrO}, w), 893 (ν_{UO}, s), 883 (ν_{CrO}, s), 871 (ν_{UO}, s), 840 (ν_{CrO}, s), 820 (ν_{CrO}, s), 801 (ν_{CrO}, s), 785 (ν_{CrO}, s), 743 (ν_{CrO}, m).

2.3. Crystallographic studies

A single crystal of $K_6[(UO_2)_4(CrO_4)_7] \cdot 6H_2O$ (1) with dimensions of $0.160 \times 0.160 \times 0.078\ mm^3$ was mounted on a glass fiber with epoxy and aligned on a Bruker SMART APEX CCD X-ray diffractometer with a digital camera. An Oxford Cryostat was used to adjust the data collection temperature to −80°C. Intensity measurements were performed using graphite monochromated Mo$K\alpha$ radiation from a sealed tube with a monocapillary collimator. SMART was used to determine the preliminary cell constants from 90 frames collected with an exposure time of 10 s, and to subsequently control the data collection. For 1, the intensities of reflections of a sphere were collected by a combination of 3 sets of exposures (frames). Each set had a different ϕ angle for the crystal and each exposure covered a range of 0.3° in ω. A total of 1800 frames were collected with an exposure time per frame of 30 s.

Determination of integral intensities and global cell refinement were performed with the Bruker SAINT (v 6.02) software package using a narrow-frame integration algorithm. An analytical absorption correction was applied, followed by a semi-empirical absorption correction using SADABS [28–30]. The program suite SHELXTL (v 5.1) was used for space group determination (XPREP), structure solution (XS), and refinement (XL) [31]. The final refinement included anisotropic displacement parameters for all atoms in 1 and a secondary extinction parameter. Some crystallographic details are listed in Tables 1 and 2 for 1. Additional details of anisotropic displacement parameters are available in the supporting CIF file.

3. Results and discussion

3.1. Syntheses

$K_6[(UO_2)_4(CrO_4)_7] \cdot 6H_2O$ (1) and $K_2[UO_2(CrO_4)_2(H_2O)] \cdot 3H_2O$ have both been prepared using mild hydrothermal reactions employing equimolar quantities of UO_3 and $K_2Cr_2O_7$. In an attempt to produce phase pure materials and to determine the subtle differences

Table 1
Crystallographic data for $K_6[(UO_2)_4(CrO_4)_7] \cdot 6H_2O$ (**1**)

Formula	$K_6[(UO_2)_4(CrO_4)_7] \cdot 6H_2O$
Formula mass (amu)	2234.82
Color and habit	Orange rhombohedron
Crystal system	Orthorhombic
Space group	$P2_12_12$ (No. 18)
a (Å)	10.9583(5)
b (Å)	22.582(1)
c (Å)	7.9552(4)
V (Å^3)	1968.6(2)
Z	2
T (°C)	–80
λ (Å)	0.71073
ρ_{calcd} ($g\,cm^{-3}$)	3.770
μ(Mo$K\alpha$) (cm^{-1})	189.92
$R(F)$ for $F_o^2 > 2\sigma(F_o^2)$[a]	0.0177
$R_w(F_o^2)$[b]	0.0410

[a] $R(F) = \sum||F_o - F_c||/\sum|F_o|$.
[b] $R_w(F_o^2) = [\sum[w(F_o^2 - F_c^2)^2]/\sum wF_o^4]^{1/2}$.

Table 2
Atomic coordinates and equivalent isotropic displacement parameters for $K_6[(UO_2)_4(CrO_4)_7] \cdot 6H_2O$ (**1**)

Atom	x	y	z	U_{eq} (Å^2)[a]
K(1)	0.0018(2)	0.1042(1)	−0.0029(2)	0.043(1)
K(2)	0.1657(1)	0.2718(1)	−0.1231(2)	0.041(1)
K(3)	0.0289(1)	0.4155(1)	−0.3828(2)	0.023(1)
U(1)	−0.0184(1)	0.2608(1)	−0.6315(1)	0.013(1)
U(2)	−0.2496(1)	0.5035(1)	−0.7289(1)	0.014(1)
Cr(1)	−1/2	1/2	−0.4049(1)	0.018(1)
Cr(2)	0.2941(1)	0.3225(1)	−0.6761(1)	0.020(1)
Cr(3)	−0.2939(1)	0.3544(1)	−0.5322(1)	0.015(1)
Cr(4)	−0.0147(1)	0.4004(1)	−0.8958(1)	0.013(1)
O(1)	−0.3839(4)	0.5242(2)	−0.5248(6)	0.039(1)
O(2)	−0.4524(4)	0.4471(2)	−0.2891(5)	0.040(1)
O(3)	0.2505(4)	0.3924(2)	−0.6792(7)	0.048(1)
O(4)	0.1780(3)	0.2785(1)	−0.7343(5)	0.019(1)
O(5)	0.4056(4)	0.3118(2)	−0.8019(5)	0.041(1)
O(6)	0.3376(3)	0.3056(2)	−0.4818(5)	0.022(1)
O(7)	−0.3316(3)	0.4097(1)	−0.6642(5)	0.020(1)
O(8)	−0.2183(3)	0.3032(1)	−0.6411(5)	0.021(1)
O(9)	−0.2079(3)	0.3783(2)	−0.3862(5)	0.026(1)
O(10)	−0.4168(3)	0.3239(2)	−0.4477(5)	0.023(1)
O(11)	0.0974(3)	0.4490(1)	−0.8987(4)	0.018(1)
O(12)	−0.1513(3)	0.4344(1)	−0.9063(5)	0.017(1)
O(13)	−0.0091(3)	0.3615(1)	−0.7211(4)	0.019(1)
O(14)	−0.0041(4)	0.3581(1)	−0.0575(4)	0.022(1)
O(15)	−0.0542(3)	0.2312(2)	−0.8330(4)	0.019(1)
O(16)	0.0174(3)	0.2917(1)	−0.4310(4)	0.018(1)
O(17)	−0.3612(3)	0.5114(2)	−0.8905(5)	0.023(1)
O(18)	−0.1328(3)	0.4939(2)	−0.5737(4)	0.020(1)
O(19)	0.1655(4)	0.5042(2)	−0.2221(4)	0.029(1)
O(20)	0.2710(4)	0.3862(2)	−0.2097(6)	0.039(1)
O(21)	0.2078(4)	0.1681(2)	0.0450(6)	0.036(1)

[a] U_{eq} is defined as one-third of the trace of the orthogonalized U_{ij} tensor.

that lead to the preferential formation of 1 or $K_2[UO_2(CrO_4)_2(H_2O)] \cdot 3H_2O$, reactions have been carried out over a wide range of times, temperatures, and water fill levels. Virtually all reaction conditions employed yielded a mixture of 1 and $K_2[UO_2(CrO_4)_2(H_2O)] \cdot 3H_2O$, however, pure 1 has been produced with the conditions specified in the experimental section. The highest yield reaction is reported in Section 2.

Reactions carried out at temperatures between 130°C and 200°C have been successful in preparing both compounds $K_6[(UO_2)_4(CrO_4)_7] \cdot 6H_2O$ (1) and $K_2[UO_2(CrO_4)_2(H_2O)] \cdot 3H_2O$, although as the temperature is increased the ratio of **1**: $K_2[UO_2(CrO_4)_2(H_2O)] \cdot 3H_2O$ generally increases. The effect of reaction duration on product yield has been less conclusive in determining the relative quantities of 1 and $K_2[UO_2(CrO_4)_2(H_2O)] \cdot 3H_2O$. Shorter reaction duration of 24 h have resulted in decreased yields of desired uranyl chromates, and have resulted in unreacted UO_3. Longer reaction times of 48–77 h have produced 1 and $K_2[UO_2(CrO_4)_2(H_2O)] \cdot 3H_2O$ with no apparent change in product ratio. The highest yields for 1 and $K_2[UO_2(CrO_4)_2(H_2O)] \cdot 3H_2O$ have been found with 1 mL millipore H_2O as the solvent, with little difference found for reactions containing increased solvent volumes up to 2 mL.

3.2. Structure of $K_6[(UO_2)_4(CrO_4)_7] \cdot 6H_2O$ (1)

The structure of 1 is formed from UO_2^{2+} cations that are bound by chromate anions to yield a pentagonal bipyramidal geometry around the uranium centers. The fundamental building units found in 1 are depicted in Fig. 1. These polyhedra are bridged by chromate anions to yield one-dimensional ${}^{1}_{\infty}[UO_2(CrO_4)_2]^{2-}$ chains. The

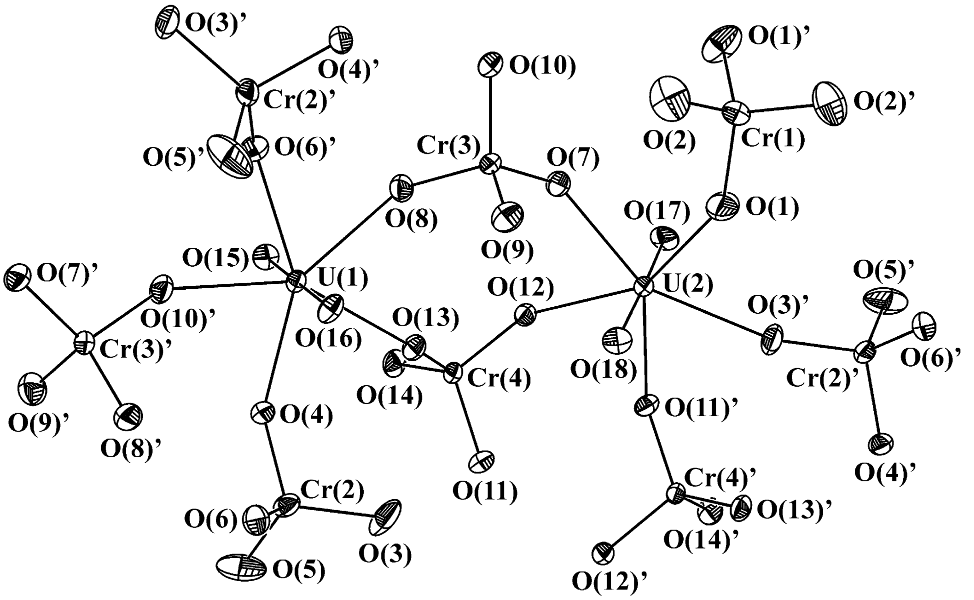

Fig. 1. A depiction of the local environments of U(1) and U(2) in $K_6[(UO_2)_4(CrO_4)_7] \cdot 6H_2O$ (**1**). 50% probability ellipsoids are shown.

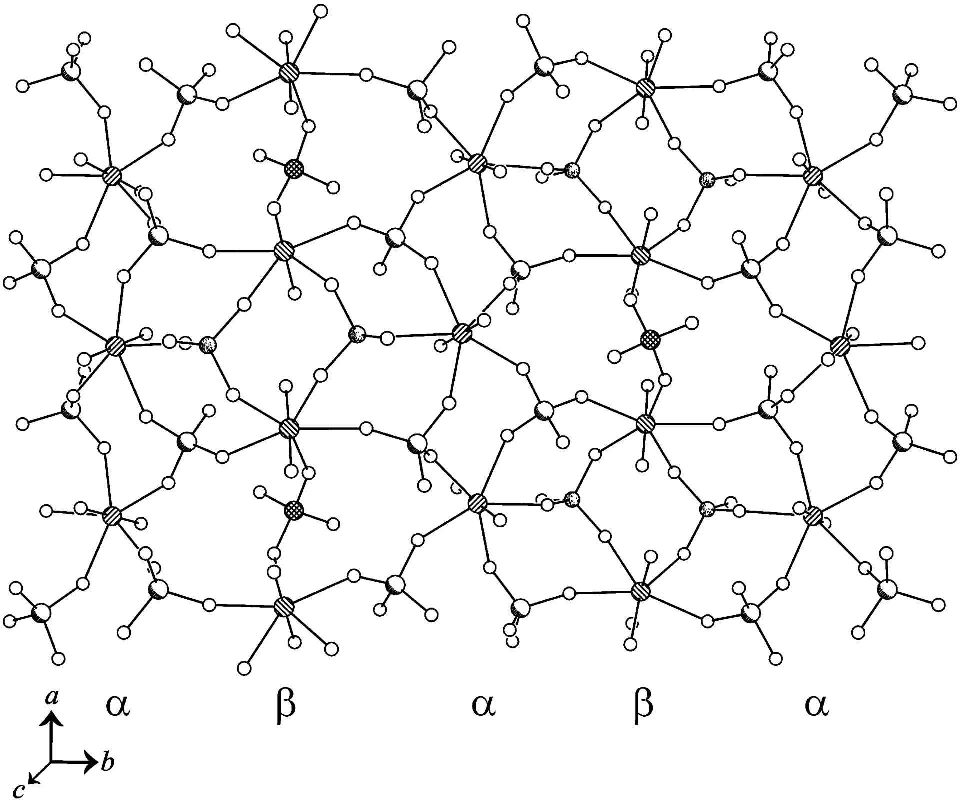

Fig. 2. A view of the two-dimensional, anionic $^{2}_{\infty}[(UO_2)_4(CrO_4)_7]^{6-}$ sheets in $K_6[(UO_2)_4(CrO_4)_7]\cdot6H_2O$ (**1**). The $^{1}_{\infty}[UO_2(CrO_4)_2]^{2-}$ α-chains and $^{1}_{\infty}[(UO_2)_2(CrO_4)_3]^{2-}$ β-chains contain $[UO_7]$ pentagonal bipyramids and $[CrO_4]$ tetrahedra.

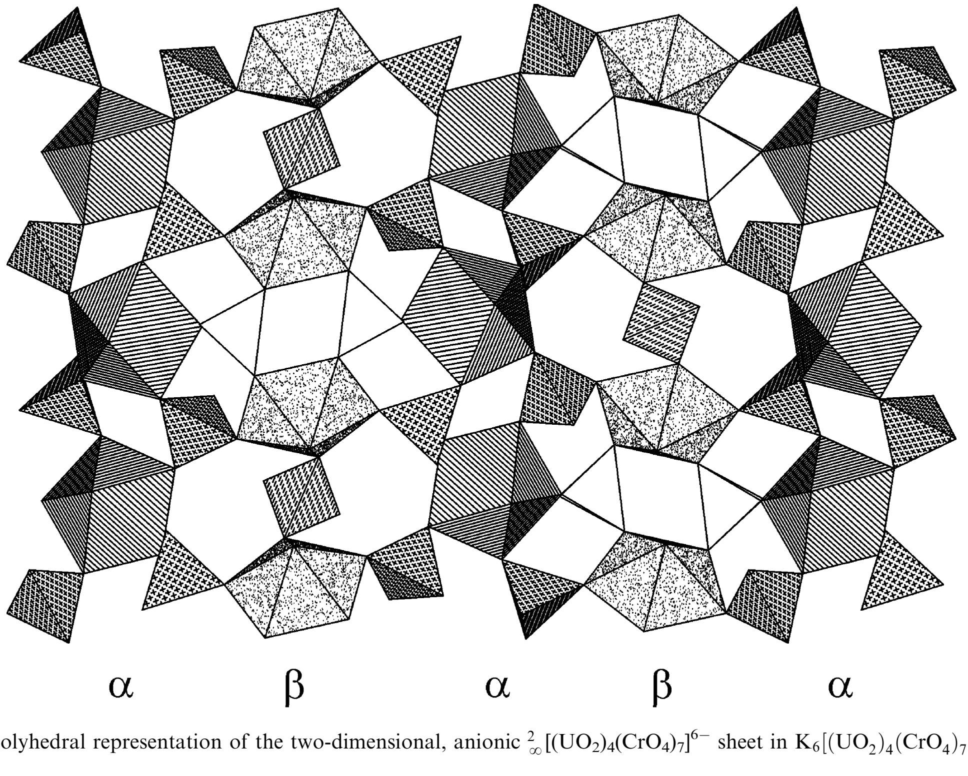

Fig. 3. A polyhedral representation of the two-dimensional, anionic $^{2}_{\infty}[(UO_2)_4(CrO_4)_7]^{6-}$ sheet in $K_6[(UO_2)_4(CrO_4)_7]6H_2O$ (**1**).

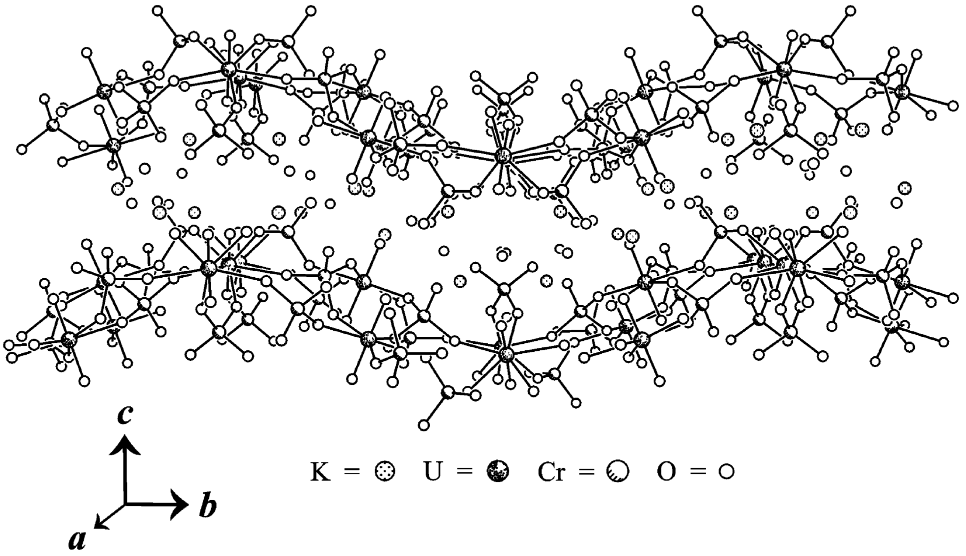

Fig. 4. An illustration of the stacking of the $^{2}_{\infty}[(UO_2)_4(CrO_4)_7]^{6-}$ layers in $K_6[(UO_2)_4(CrO_4)_7] \cdot 6H_2O$ (**1**). K^+ cations are found both intra- and interlayer.

chains are similar to the $^{1}_{\infty}[UO_2(CrO_4)_2(H_2O)]^{2-}$ chains found in the previously reported one-dimensional uranyl chromate, $K_2[UO_2(CrO_4)_2(H_2O)] \cdot 3H_2O$ [8]. These chains are condensed with the loss of the coordinated water molecules into two-dimensional $^{2}_{\infty}[(UO_2)_4(CrO_4)_7]^{6-}$ layers parallel to the [*ab*] plane with additional one-dimensional $^{1}_{\infty}[(UO_2)_2(CrO_4)_3]^{2-}$ chains. K^+ cations and occluded water molecules separate the layers from one another. A representation of the two-dimensional layers normal to the *c*-axis can be seen in Fig. 2. The U(1) pentagonal bipyramidal polyhedra are linked with the Cr(2) and Cr(3) tetrahedra into chains, referred to as α-chains, reminiscent of those found in $K_2[UO_2(CrO_4)_2(H_2O)] \cdot 3H_2O$ [8]. The main difference in these α-chains found in 1 is the lack of the coordinated water molecule. The second type of chains are formed with the U(2) polyhedra and will be called β-chains. The U(2) atoms are also found in pentagonal bipyramidal environments and are connected with chromate anions into one-dimensional β-chains that run along the *a*-axis. In these β-chains composed of U(2) polyhedra, the connectivity of uranyl units alternates between bridging by one Cr(1) or two Cr(4) tetrahedra. These α- and β-chains and the overall sheet topology created from their condensation is depicted in polyhedral form in Fig. 3 as viewed down the *c*-axis.

The overall two-dimensional $^{2}_{\infty}[(UO_2)_4(CrO_4)_7]^{6-}$ layers found in 1 are formed from the linking of the α- and β-chains as shown in Fig. 3. The Cr(2), Cr(3), and Cr(4) tetrahedra all bridge one additional oxygen in an inter-chain fashion, making them tridentate, leading to the connectivity of the α- and β-chains into the new type of two-dimensional layers found in the *ab* plane of 1 [32,33]. These layers are separated by three crystallographically unique potassium cations, that balance charge, and also by water molecules of hydration as shown in Fig. 4. The $K^+ \cdot O$ bond lengths are typical with distances ranging from 2.643(4) to 3.232(4) Å.

Table 3
Selected bond distances (Å) and angles (°) for $K_6[(UO_2)_4(CrO_4)_7] \cdot 6H_2O$ (**1**)

Bond lengths (Å)			
U(1)–O(4)	2.337(3)	Cr(1)–O(1) × 2	1.681(4)
U(1)–O(6)′	2.356(3)	Cr(1)–O(2) × 2	1.596(4)
U(1)–O(8)	2.391(3)	Cr(2)–O(3)	1.648(4)
U(1)–O(10)′	2.302(3)	Cr(2)–O(4)	1.679(3)
U(1)–O(13)	2.385(3)	Cr(2)–O(5)	1.598(4)
U(1) = O(15)	1.781(3)	Cr(2)–O(6)	1.662(4)
U(1) = O(16)	1.785(3)	Cr(3)–O(7)	1.677(3)
U(2)–O(1)	2.240(4)	Cr(3)–O(8)	1.662(3)
U(2)–O(3)′	2.384(3)	Cr(3)–O(9)	1.595(4)
U(2)–O(7)	2.359(3)	Cr(3)–O(10)	1.659(4)
U(2)–O(11)′	2.399(3)	Cr(4)–O(11)	1.647(3)
U(2)–O(12)	2.364(3)	Cr(4)–O(12)	1.684(3)
U(2) = O(17)	1.783(3)	Cr(4)–O(13)	1.645(3)
U(2) = O(18)	1.792(3)	Cr(4)–O(14)	1.607(3)
Angles (°)			
O(15) = U(1) = O(16)	179.1(1)	O(17) = U(2) = O(18)	177.3(2)

In 1, the nearly linear uranyl groups have average U = O bond lengths of 1.785(3) Å and bond angles of 179.08(14)° and 177.3(2)° for U(1) and U(2), respectively. In addition, the equatorial oxygen atoms around the $[UO_7]$ pentagonal bipyramids contain U–O distances ranging from 2.240(4) to 2.399(3) Å. The bond lengths for the $[CrO_4]$ tetrahedra are within normal ranges, with a clear distinction displayed for bridging or terminal Cr–O bond lengths. For the chromates, the terminal oxygen atoms have Cr–O distances ranging from 1.595(4) to 1.607(3) Å, and the bridging oxygens have Cr–O bond lengths between 1.645(3) and 1.684(3) Å. A more detailed listing of bond distances and angles is given in Table 3. Bond valence sum calculations performed on the uranium and chromium centers in 1 provide values consistent with U(VI) and Cr(VI); the values for U(1) and U(2) are 6.08 and 6.09, respectively, while the values for the four unique chromium sites range from 5.95 to 6.13 [34–36].

Acknowledgments

This work was supported by the Department of Energy, Office of Basic Energy Sciences, Heavy Elements Program (Grant No. DE-FG02-01ER15187).

Auxiliary Material: Further details of the crystal structure investigation may be obtained from the Fachinformationzentrum Karlsruhe, D-76344 Eggenstein-Leopoldshafen, Germany (Fax: (+49)7247-808-666; mailto: crysdata@fiz-karlsruhe.de) on quoting depository numbers CSD 413416.

References

[1] X. Wang, J. Huang, A.J. Jacobson, J. Am. Chem. Soc. 124 (2002) 15190.
[2] S.V. Krivovichev, P.C. Burns, Inorg. Chem. 41 (2002) 4108.
[3] N.W. Alcock, S. Esperas, J. Chem. Soc. Dalton Trans. 9 (1977) 893.
[4] D. Atencio, R. Neumann, A.J.G.C. Silva, Y.P. Mascarenhas, Can. Miner. 29 (1991) 95.
[5] J. Borene, F. Cesbron, Bull. Soc. Fr. Mineral. Crystallogr. 93 (1970) 426.
[6] R.E. Sykora, S.M. McDaniel, D.M. Wells, T.E. Albrecht-Schmitt, Inorg. Chem. 41 (2002) 5126.
[7] R.E. Sykora, D.M. Wells, T.E. Albrecht-Schmitt, Inorg. Chem. 41 (2002) 2304.
[8] N.V. Boiko, E.Yu. Grigor'eva, V.N. Serezhkin, Zh. Neorg. Khim. 30 (1985) 717.
[9] V.N. Serezhkin, N.V. Boiko, L.B. Serezhkina, Radiokhimiya 23 (1981) 868.
[10] M.A. Soldatkina, L.B. Serezhkina, V.N. Serezhkin, Zh. Neorg. Khim. 27 (1982) 1765.
[11] N.V. Boiko, L.B. Serezhkina, V.N. Serezhkin, Radiokhimiya 27 (1985) 183.
[12] N.V. Kuchumova, L.B. Serezhkina, V.N. Serezhkin, Radiokhimiya 30 (1988) 317.
[13] V.N. Serezhkin, L.B. Serezhkina, Zh. Neorg. Khim. 30 (1985) 2039.
[14] N.V. Boiko, V.N. Serezhkin, Zh. Neorg. Khim. 29 (1984) 1333.
[15] O.L. Vdovina, L.B. Serezhkina, V.N. Serezhkin, N.V. Boiko, Radiokhimiya 25 (1983) 345.
[16] L.M. Kovba, V.K. Trunov, A.I. Grigor'ev, Zh. Strukt. Khim. 6 (1965) 919.
[17] Yu.N. Mikhailov, Yu.E. Gorbunova, L.B. Serezhkina, V.N. Serezhkin, Zh. Neorg. Khim. 42 (1997) 734.
[18] L.B. Serezhkina, V.K. Trunov, L.N. Kholodkovskaya, N.V. Kuchumova, Koord. Khim. 16 (1990) 1288.
[19] V.N. Serezhkin, N.V. Boiko, V.K. Trunov, Zh. Strukt. Khim. 23 (1982) 121.
[20] S.V. Krivovichev, P.C. Burns, Z. Krystollogr. 218 (2003) 568.
[21] Yu.N. Mikhailov, I.M. Orlova, G.V. Podnebesnova, V.G. Kuznetsov, R.N. Shchelokov, Koord. Khim. 2 (1976) 1681.
[22] Yu.N. Mikhailov, Yu.E. Gorbunova, E.A. Demchenko, L.B. Serezhkina, V.N. Serezhkin, Zh. Neorg. Khim. 44 (1999) 1444.
[23] L.B. Serezhkina, V.N. Serezhkin, Koord. Khim. 17 (1991) 1005.
[24] V.N. Serezhkin, M.A. Soldatkina, V.A. Efremov, V.K. Trunov, Koord. Khim. 7 (1981) 629.
[25] Yu.N. Mikhailov, Yu.E. Gorbunova, E.A. Demchenko, L.B. Serezhkina, V.N. Serezhkin, Zh. Neorg. Khim. 43 (1998) 971.
[26] Yu.N. Mikhailov, Yu.E. Gorbunova, E.A. Demchenko, L.B. Serezhkina, V.N. Serezhkin, Zh. Neorg. Khim. 43 (1998) 1831.
[27] V.N. Serezhkin, V.K. Trunov, Kristallography 26 (1981) 301.
[28] SADABS. Program for absorption correction using SMART CCD based on the method of Blessing: R.H. Blessing, Acta Crystallogr. A 51 (1995) 33.
[29] F.Q. Huang, J.A. Ibers, Inorg. Chem. 40 (2001) 2602.
[30] T.E. Albrecht-Schmitt, P.M. Almond, R.E. Sykora, Inorg. Chem. 42 (2003) 3788.
[31] G.M. Sheldrick, SHELXTL PC, Version 5.0, An Integrated System for Solving, Refining, and Displaying Crystal Structures from Diffraction Data; Siemens Analytical X-ray Instruments, Inc, Madison, WI, 1994.
[32] (a) P.C. Burns, R.C. Ewing, F.C. Hawthorne, Can. Mineral. 35 (1997) 1551;
(b) P.C. Burns, in: P.C. Burns, R. Finch, (Eds.), Uranium: Mineralogy, Geochemistry and the Environment, Mineralogical Society of America: Washington, DC, 1999 (Chapter 1).
(c) P.C. Burns, M.L. Miller, R.C. Ewing, Can. Mineral. 34 (1996) 845.
[33] (a) S.V. Krivovichev, P.C. Burns, Solid State. Sci. 373 (2003) 5 For some examples of newly recognized uranyl sheet topologies see.
(b) J.-Y. Kim, A.J. Norquist, D. O'Hare, Chem. Mater. 15 (2003) 1970.
(c) P.C. Burns, K.M. Deely, Can. Mineral. 40 (2002) 1579.
(d) S.V. Krivovichev, C.L. Cahill, P.C. Burns, Inorg. Chem. 41 (2002) 34.
(e) S.V. Krivovichev, P.C. Burns, Inorg. Chem. 41 (2002) 4108.
(f) A.J. Norquist, P.M. Thomas, M.B. Doran, D. O'Hare, Chem. Mater. 14 (2002) 5179.
(g) M. Saadi, C. Dion, F. Abraham, J. Solid State Chem. 72 (2000) 150.
(h) P.C. Burns, F.C. Hill, Can. Mineral. 38 (2000) 163.
(i) C.L. Cahill, P.C. Burns, Am. Mineral. 85 (2000) 1294.
(j) S.V. Krivovichev, P.C. Burns, Can. Mineral. 38 (2000) 847.
(k) P.C. Burns, Am. Mineral. 84 (1999) 1661.
(l) F.C. Hill, P.C. Burns, Can. Mineral. 37 (1999) 1283.
(m) P.C. Burns, J.M. Hanchar, Can. Mineral. 37 (1999) 1483.
(n) P.C. Burns, Can. Mineral. 36 (1998) 187.
(o) A. Guesdon, B. Raveau, Chem. Mater. 10 (1998) 3471.
[34] I.D. Brown, D. Altermatt, Acta Crystallogr. B 41 (1985) 244.
[35] N.E. Brese, M. O'Keeffe, Acta Crystallogr. B 47 (1991) 192.
[36] P.C. Burns, R.C. Ewing, F.C. Hawthorne, Can. Mineral. 35 (1997) 1551.